LC-PHSM-2004-011
July 1, 2004

A Study of Triple Gauge Boson Couplings in W-pair Production at the Linear Collider using Transversely Polarized Beams

Filip Franco-Sollova
Deutsches Elektronen-Synchrotron DESY
Notkestraße 85, 22607, Hamburg, Germany

Abstract

The sensitivity of the future Linear Collider for measuring triple gauge couplings in W-pair production using transversely polarized beams is studied. The results are compared with the case of longitudinally polarized beams, showing the advantage of longitudinal polarization over transverse polarization. Also the sensitivity to contributions coming from longitudinal W bosons are studied by considering the azimuthal distribution asymmetry present in the case of transversely polarized beams.

1 Introduction

Precision measurements of the gauge boson properties can help either to confirm the $SU(2)_L \otimes U(1)_Y$ structure of the electroweak sector of the Standard Model (SM), or to observe deviations from the SM coming from new physics. Extensions of the SM like Supersymmetry (SUSY) models would also manifest themselves as loop corrections which could be measurable at an e^+e^- Linear Collider with a center-of-mass energy of 500 GeV [1]. On the other hand, the couplings between gauge bosons are sensitive to models of strong electroweak symmetry breaking; in addition, high precision measurements will be useful to increase the confidence for the extrapolation of the couplings to high scales in order to test theories of grand unification.

The production of W-pairs in electron-positron annihilation offers the possibility to test the WWZ and $WW\gamma$ Triple Gauge Boson Couplings (TGCs). Beam polarization gives the advantage of increasing the sensitivity to deviations from the SM and also permits to disentangle different contributions.

In this study the option of transverse beam polarization is considered. Once longitudinal beam polarization is realized, it is possible to use spin rotators to achieve transverse polarization [2]. The sensitivity to anomalous TGCs obtained with transverse beam polarization is compared with the case of longitudinal beam polarization. This topic has been already addressed in a comprehensive way by Nagel et. al. in [3]. The difference between the two studies will be explained in Section 5. In addition, the potential to study the physics of longitudinal W bosons is outlined.

1.1 Triple Gauge Boson Couplings

Figures 1(a) and 1(b) show the Feynman diagrams for on-shell W-pair production. Fig.1(a) corresponds to the ν-exchange t-channel diagram, and Fig.1(b) shows the s-channel diagram containing the three gauge boson vertex, which is sensitive to anomalous TGC. The three gauge boson couplings WWV ($V = Z$ or γ) are parameterized by the effective Lagrangian [4]

$$\begin{aligned}
\frac{\mathcal{L}_{WWV}}{ig_{WWV}} &= g_1^V V^\mu (W^-_{\mu\nu} W^{+\nu} - W^+_{\mu\nu} W^{-\nu}) + \kappa_V W^-_\mu W^+_\nu V^{\mu\nu} \\
&+ \frac{\lambda_V}{M_W^2} V^{\mu\nu} W^{+\rho}_\mu W^-_{\rho\nu} - i g_4^V W^-_\mu W^+_\nu (\partial^\mu V^\nu + \partial^\nu V^\mu) \\
&+ i g_5^V \varepsilon^{\mu\nu\rho\sigma} \left[(\partial^\rho W^-_\mu) W^+_\nu - W^-_\mu (\partial^\rho W^+_\nu) \right] V_\sigma \\
&+ \frac{\tilde{\kappa}_V}{2} W^-_\mu W^+_\mu \varepsilon^{\mu\nu\rho\sigma} V_{\rho\sigma} + \frac{\tilde{\lambda}_V}{2M_W^2} W^-_{\rho\mu} W^{+\mu}_\nu V_{\alpha\beta},
\end{aligned}$$

here $U_{\mu\nu} = \partial_\mu U_\nu - \partial_\nu U_\mu$, with $U = W^\pm, Z, \gamma$. In the SM at tree level the values of the parameters are fixed. One has $g_1^V = k_V = 1$, and the other couplings are equal to zero. The couplings g_1^V, k_V, λ_V and g_5^V are CP conserving, while $g_4^V, \tilde{k}_V, \tilde{\lambda}_V$ violate CP.

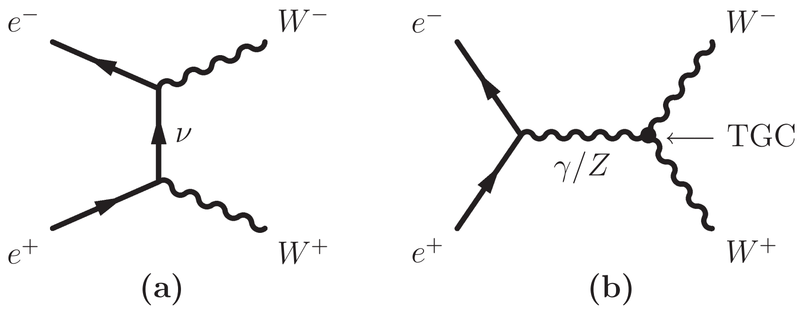

Figure 1: Feynman diagrams which contribute to the W-pair production in e^+e^--annihilation. Fig. 1(a) shows the ν-exchange t-channel diagram. Fig. 1(b) corresponds to the s-channel diagram containing the TGC.

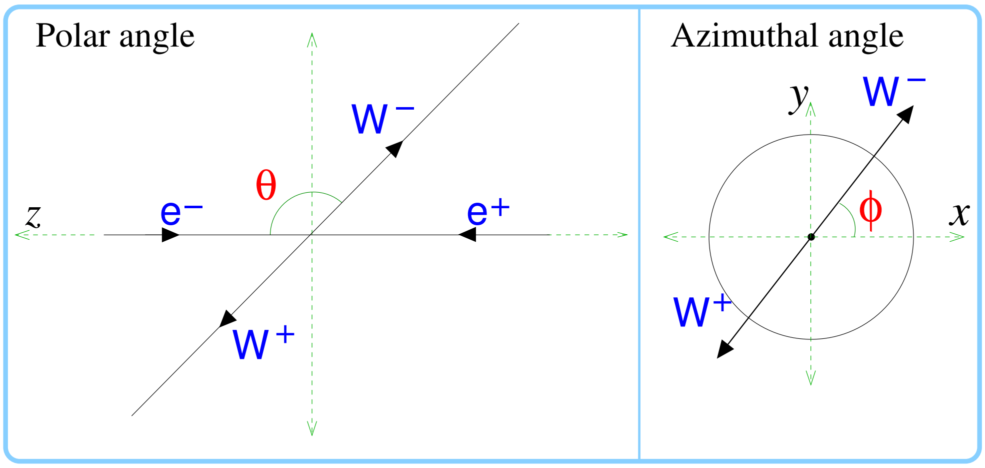

Figure 2: W-pair production angles: The polar angle θ (the angle between e^- and W^-), and the azimuthal angle ϕ (in the x-y-plane).

2 Transverse Polarization

In the case of unpolarized or longitudinally polarized beams the differential cross section depends on the W-pair production polar angle θ between the electron and the W^- (Fig. 2), but it is independent of the azimuthal angle ϕ, in the x-y-plane. A dependency on the azimuthal angle is present only in the case of transverse beam polarization. The explicit dependency on the angles will be discussed in the following.

Consider the electron density matrix $\rho_{\sigma\sigma'}$ in the helicity basis

$$\rho_{\sigma\sigma'} = \frac{1 + \vec{\sigma} \cdot \vec{P}}{2} = \frac{1}{2} \begin{bmatrix} 1 + P_L & P_T e^{-i\phi} \\ P_T e^{-i\phi} & 1 - P_L \end{bmatrix}, \tag{1}$$

where $\vec{P} = (P_T \cos\phi, P_T \sin\phi, P_L)$, P_L and P_T denote the magnitude of the longitudinal polarization and the transverse polarization, and $\vec{\sigma}$ are the Pauli matrices. Consider also the helicity amplitudes $M_{\sigma\overline{\sigma}}$ for the process $e^+e^- \longrightarrow W^+W^-$ ($\sigma,\overline{\sigma}$ are the helicities of the electron and the positron respectively). Then, the square of the matrix element for W-pair production is given by

$$\overline{|M|}^2 = \sum \rho_{\sigma\sigma'}\overline{\rho}_{\bar{\sigma}\bar{\sigma}'}M_{\sigma\bar{\sigma}}M^*_{\sigma'\bar{\sigma}'} \tag{2}$$

Only the amplitudes M_{-+} and M_{+-} are different from zero in the limit of vanishing electron mass. Using the explicit form of the density matrix (1) gives[6]:

$$\begin{aligned} \frac{d\sigma}{d\Omega} \propto \overline{|M|^2} &= \frac{1}{4}(1-P_LP'_L)(|M_+|^2+|M_-|^2) + \frac{1}{4}(P_L-P'_L)(|M_+|^2-|M_-|^2) \\ &\quad -\frac{1}{2}(P_TP'_T)\left[\cos(2\phi)\,\mathrm{Re}(M_+M_-^*) + \sin(2\phi)\,\mathrm{Im}(M_+M_-^*)\right], \end{aligned} \tag{3}$$

where $M_- = M_{-+}$ and $M_+ = M_{+-}$. In this expression one can appreciate the ϕ-dependence of $d\sigma/d\Omega$ in the presence of transverse polarization. Three situations can be distinguished:

a) **No polarization** ($P_L = P_T = 0$): When no beam polarization is present the contribution coming from $|M_+|^2 + |M_-|^2$ is measured.

b) **Longitudinal polarization**: In the presence of longitudinal polarization one is again sensitive to $|M_+|^2 - |M_-|^2$ in addition to $|M_+|^2 + |M_-|^2$.

c) **Transverse Polarization**: In the case of transverse polarization ($P_TP'_T \neq 0$) contributions from $\mathrm{Re}(M_+M_-^*)$ and $\mathrm{Im}(M_+M_-^*)$ are measured. The the ϕ-distribution deviates from the flat shape present when the beams are not polarized or longitudinally polarized (Fig. 3). In the SM only CP-conserving couplings occur. In this case $\mathrm{Im}(M_+M_-^*) = 0$ and only the term containing $\cos 2\phi$ contributes.

Figure 4 shows $\cos\theta$-distributions of the W^- bosons for transverse and longitudinal beam polarization for SM couplings and for $\tilde{k}_Z = 1$. Here one can observe the change of the cross section for anomalous TGCs.

The size of the contribution from $\mathrm{Re}(M_+M_-^*)$ in Eq. 3 can be estimated by the azimuthal asymmetry $d(\sigma A_T)/d\cos\theta$:

$$\begin{aligned} \frac{d(\sigma A_T)}{d\cos\theta} &= \int_{-\pi}^{\pi} \frac{d\sigma}{d\Omega}\cos 2\phi\, d\phi \\ &= \frac{\beta_W}{64\pi s} 2\,\mathrm{Re}(M_+M_-^*), \end{aligned}$$

where $\beta_W = \sqrt{1-4M_W^2/s}$ and $s = 4E_b^2$, with E_b being the beam energy. The azimuthal asymmetry has an interesting feature: while the contribution of the $W_L^+W_L^-$ final state to the total cross section is very small, it is the one which completely dominates in the azimuthal asymmetry. The contributions from the state in which W^+ has transverse polarization and W^- is longitudinal ($W_T^- W_L^+$) and the contribution coming from the ($W_L^- W_T^+$) state mutually cancel. In this sense, the azimuthal asymmetry could be used to study the physics of longitudinal W bosons without analyzing the final state polarization[6].

3 Analysis

3.1 Frame of the Study

The following conditions are assumed for this study: a center-of-mass energy of 500 GeV, a luminosity L of 500 fb^{-1} and transverse beam polarization (80% right handed electrons and 60% left handed positrons). The Monte Carlo (MC) samples are generated with WHIZARD [7], including initial state radiation (ISR) and beamstrahlung. The diagrams which contribute to the W-pair production are the t-channel ν exchange and the s-channel γ and Z exchange (Fig. 2). The WHIZARD input file for the case of transverse polarization is given in Appendix B. Only the semileptonic decay channel, $e^+e^- \longrightarrow W^+W^- \longrightarrow \mu\bar{\nu}_\mu q_1\bar{q}_2$, where the charged lepton is a muon is considered. The three decay channels for W-pair production, the leptonic, the semileptonic and the hadronic, have branching ratios of 0.106, 0.439 and 0.456 respectively[5]. For the decay channel considered in this study the branching ratio corresponds to 1/3 of the total semileptonic branching ratio, and therefore, the sensitivity obtained in this study is roughly $\sqrt{3}$ times the sensitivity for the semileptonic channel.

3.2 Fit Method and Construction of Reference Distributions

The sensitivity to deviations from the SM value for a generic coupling constant $\alpha \in \{g_1^V, \kappa_V, \lambda_V, g_4^V, g_5^V, \tilde{\kappa}_V, \tilde{\lambda}_V\}$ ($V = \gamma$ or Z), is quantified by means of the 1σ-bound, defined as the value of α for which the SM and the anomalous coupling distributions are distinguishable at the 1σ level. The smaller the 1σ-bound is, the highest the sensitivity to effects beyond the SM is.

To obtain the 1σ-bound, angular distributions ($\cos\theta$, ϕ and two-dimensional ($\cos\theta, \phi$)) for different values of the parameter α are compared with the ones assumed in the SM using the χ^2 method.[1] The 1σ-bound for anomalous values of α, is determined by the condition $\Delta\chi^2(\alpha_{1\sigma}) = 1$, where $\Delta\chi^2 = \chi^2 - \chi^2_{min}$; here χ^2_{min} corresponds to the SM case. The construction of a reference distribution for a given value of α is described below.

[1]Given two distribution histograms with *i-th* bin contents m_i and n_i, one defines:

$$\chi^2 = \sum_i \left(\frac{m_i - n_i}{\sqrt{m_i}} \right)^2$$

.

It is impossible to generate MC events for each required value of the parameter α, but one can construct a reference distribution for a given value of α assuming a quadratic behavior of the cross section on the coupling constants for each bin of the distribution. This is motivated by the linear occurrence of the coupling constants in (1). For the construction of the reference distributions 3 sets of MC events for different values of α: $\alpha_0, \alpha_1, \alpha_2$ are used. The events are generated with WHIZARD using the conditions described in 3.1. Let $n_i(\alpha)$ denote the bin content of the *i-th* bin from an angular distribution histogram for a given value of the parameter α, and let α_1 be the SM value of α. A parabola $n_i(\alpha)$ which contains the points $n_i(\alpha_0), n_i(\alpha_1)$ and $n_i(\alpha_2)$ is constructed for each bin of the angular distribution histograms. In this way, one can obtain a reference distribution with bin contents $n_i(\alpha)$ just by inserting the desired value of α. The procedure employed to compute the 1σ-bound and to verify the method is described in appendix A.

The values of α_0 and α_2 have to be carefully chosen in order to obtain distributions which significantly differ from the SM one. α_0 and α_2 are shifted from the SM value by $\Delta\alpha = |\alpha_1 - \alpha_{0,2}|$ ranging from 0.15 to 1, depending on how fast the cross section varies with a given parameter α.

3.3 Azimuthal Asymmetry

The sensitivity to deviations from the SM value for the azimuthal asymmetry can be obtained with the same method described in 3.2. In this case the integrated azimuthal asymmetry σA_T is studied:

$$\sigma A_T = \int_{-1}^{\cos\theta'} \frac{d(\sigma A_T)}{d\cos\theta} d\cos\theta \tag{4}$$

In order to obtain the maximum sensitivity to σA_T it is necessary to find the value of $\cos\theta'$ at which the significance $\sigma A_T/\Delta(\sigma A_T)$ is large (Figures 5 and 6). Here the error $\Delta(\sigma A_T)$ is given by the statistical error of the ϕ-distribution. If the whole range of $\cos\theta'$ is considered, then the contribution from the t-channel dominates over the s-channel one as one approaches $\cos\theta' = 1$. Here the cross section is larger, and the effects of the asymmetry, which come from the s-channel, are diminished.

The value of σA_T (Eq. 4) is obtained in the following way: A ϕ-distribution histogram is generated employing the cut $-1 \leq \cos\theta \leq \cos\theta'$, and finally σA_T is computed as $\sigma A_T = \sum_i n_i \cos 2\phi_i$, where n_i is the *i-th* bin content of the ϕ-distribution and ϕ_i is the value of ϕ in the middle of the *i-th* bin.

4 Results

The 1σ-bound to anomalous TGCs for the case of transverse beam polarization is shown in Table 1 for the $\cos\theta$ and ϕ observables as well as for 2-D $\cos\theta - \phi$ distributions. From the entries in Table 1 it can be concluded that for this beam polarization mode the $\cos\theta$-distribution offers the best possibility to detect the existence of anomalous TGC. The 1σ-bound ranges from 1.0×10^{-3} for κ_γ, to 39.0×10^{-3} for $\tilde{\kappa}_\gamma$. Similar values are obtained for the $\cos\theta-\phi$ distribution, while the values for the ϕ distribution are typically a factor 2-3 larger. Thus the $\cos\theta$ distribution is equivalent in the cases of unpolarized and transversely polarized beams. These results are obtained from binning conditions which satisfy the tests described at the end of this section. The bin size has to be a compromise between the finite number of events (luminosity) employed in this study and a reasonable small bin width in order to perform a proper χ^2 fit.

The 1σ-bound obtained for the cases of transverse and longitudinal beam polarization from the $\cos\theta$ distribution is shown in Table 2. For longitudinal beam polarization there is no ϕ-angle dependence of the cross section (Sec. 2). The 1σ-bound takes values between 0.4×10^{-3} and 21.0×10^{-3} for κ_γ and $\tilde{\kappa}_\gamma$ respectively.

Table 2 presents in addition 1σ-bound for the azimuthal asymmetry σA_T. The smallest values of the 1σ-bound are obtained from longitudinally polarized beams (80%,-60%) since already small deviations from the SM for the corresponding coupling constant lead to the required 1σ deviations of the cross section. For longitudinal beam polarization the contribution from the t-channel is strongly suppressed for the case of right-handed electrons and left-handed positrons; this fact allows to have a cleaner s-channel signal. For transverse polarization, the 1σ-bound for the azimuthal asymmetry is larger than the 1σ-bound for the angular distributions, as expected. The azimuthal asymmetry is computed for $-1 \leq \cos\theta \leq 0.5$ in order to have a large significance.

In order to verify the results for each coupling constant α, the spread of the fitted values of 10 SM MC samples of 50 fb^{-1} is obtained and compared to the 1σ-bound. The fit of the 10 SM samples was made using the scaled reference curve employed to compute the 1σ-bound (see 3.2 and appendix A). For instance, in the case of anomalous $\tilde{k}_Z$, for the $\cos\theta$-distribution the ratio of the value of the 1σ-bound and the spread of the fitted samples is 1.01. For the ϕ and $\cos\theta-\phi$ distributions the corresponding ratio is 1.04 and 1.09 respectively. The statistical compatibility of the computed 1σ-bound and the spread of the fitted values of the 10 MC samples, namely, the fact that both numbers almost coincide, is an indication for the consistency of the method employed.

5 Summary and Conclusion

Transverse beam polarization can not compete with longitudinal polarization regarding sensitivity to anomalous TGCs. The results obtained (Table 2) show that the largest sensitivity is observed for the case of longitudinal beam polarization for each coupling constant. The suppression of the t-channel ν-exchange for the case of longitudinal polarization gives the advantage over the other beam polarization modes. The superiority of longitudinal beam polarization over transverse polarization pointed out in this study is compatible with results obtained in a similar study presented in [3]. There the method of optimal observables is employed taking into account the angles of the decay products from the W bosons. In addition, the simultaneous fit of several coupling constants in [3] provides more information than the one-parameter fit employed in this study.

Aknowledgments

Thanks to Klaus Desch, Wolfgang Menges and Roman Pöschl for their helpful comments and suggestions.

References

[1] J. A. Aguilar-Saavedra *et al.* [ECFA/DESY LC Physics Working Group Collaboration], "TESLA Technical Design Report Part III: Physics at an e^+e^- Linear Collider", arXiv:hep-ph/0106315.

[2] For the employment of spin rotators at e.g. HERA see:
E. Gianfelice, "First polarization studies at HERA with 3 spin rotators", DESY-HERA-03-18

[3] M. Diehl, O. Nachtmann and F. Nagel, "Probing triple gauge couplings with transverse beam polarisation in $e^+e^- \to W^+W^-$", Eur. Phys. J. C **32** (2003) 17 [arXiv:hep-ph/0306247].

[4] K. Hagiwara, R. D. Peccei, D. Zeppenfeld and K. Hikasa, "Probing the Weak Boson Sector in $e^+e^- \to W^+W^-$", Nucl. Phys. B **282** (1987) 253.

[5] K. Hagiwara *et al.* [Particle Data Group Collaboration], "Review Of Particle Physics", Phys. Rev. D **66** (2002) 010001.

[6] J. Fleischer, K. Kolodziej and F. Jegerlehner, "Transverse versus longitudinal polarization effects in $e^+e^- \to W^+W^-$", Phys. Rev. D **49** (1994) 2174.

[7] W. Kilian, WHIZARD. A generic Monte-Carlo integration and event generation package for multi-particle processes(MANUAL), LC-TOOL-2001-039.

Appendix A

1) Procedure Employed to Compute the 1σ-bound

(a) Constructing reference distributions

i. MC event distributions for a given observable for 3 different values of α (for example $\alpha_0 = -1$, $\alpha_1 = \alpha_{SM} = 0$ and $\alpha_2 = 1$) are generated.

ii. Let $n_i(\alpha)$ denote the bin content of the *i-th* bin from the distribution histogram for the observable O for a given value of the parameter α. For each one of the bins of the 3 MC distributions a parabola $n_i(\alpha) = A\alpha^2 + B\alpha + C$ which contains the set of points $\{(\alpha_0, n_i(\alpha_0)), (\alpha_1, n_i(\alpha_1)), (\alpha_2, n_i(\alpha_2))\}$ is constructed.

(b) Determining the 1σ sensitivity limit

i. The SM ($\alpha = 0$) reference distribution is compared with distributions for $\alpha \neq 0$ (α is changed in discrete steeps of proper size) by the χ^2 method. The $\alpha \neq 0$ distribution is obtained with the aid of the parabolae constructed in 1(a)ii.

ii. The value of α for which $\Delta\chi^2 = \chi^2 - \chi^2_{min} = \chi^2 = 1$ (a vanishing error in the determination of the SM distribution, $\chi^2_{min} = 0$, is considered) is taken as the 1σ-bound.

2) Procedure Employed to Verify the Method

(a) 10 statistically independent SM MC distributions with $L = 50\text{fb}^{-1}$ are generated.

(b) Each one of the 10 distributions are compared with the scaled reference distributions obtained in 1(a)ii. For this, α is changed again in discrete steeps until $\min\{\chi^2(\alpha)\} = \chi^2(\alpha_{min})$ is found, and the value of $\alpha = \alpha_{min}$ is associated to the corresponding distribution.

(c) The fitted values of α found in step 2(b) are filled into an histogram and the width of the distribution is computed.

(d) This width has to be statistically compatible with the 1σ limit found in 1(b)ii, i.e. no more than 31,7 % of the values should be found outside the 1σ-bound. In this case, the width of the distributions obtained in 2(c) and the 1σ-bound for a given observable coincide.

Appendix B

WHIZARD input file for transverse polarization.

```
 &process_input
 process_id = "mvmdu,mvmsc,dumvm,scmvm"
 sqrts = 500
 luminosity = 500
 polarized_beams = T
 structured_beams = T
 /
!>>>>>>>>>>>>>>>>>>>>>>>>>>>>>
 &integration_input
 /
!>>>>>>>>>>>>>>>>>>>>>>>>>>>>>
 &simulation_input
 write_events = T
 write_events_format = 20
 write_events_raw = F
 keep_beam_remnants = T
 /
!>>>>>>>>>>>>>>>>>>>>>>>>>>>>>
 &diagnostics_input
 /
!>>>>>>>>>>>>>>>>>>>>>>>>>>>>>
 &parameter_input
 g1a = 1.
 g1z = 1.
 ka = 1.
 kz = 1.
 la = 0.
 lz = 0.
 g4a = 0.
 g4z = 0.
 g5a = 0.
 g5z = 0.
 k5a = 0.
 k5z = 0.
 l5a = 0.
 l5z = 0.
 /
!>>>>>>>>>>>>>>>>>>>>>>>>>>>>>
 &beam_input
 particle_name = "e-"
 vector_polarization = T
 polarization = 0 0.8 0
 ISR_on = T
 ISR_alpha = 0.0072993
 ISR_m_in = 0.000511
 CIRCE_on = T
 CIRCE_acc = 2
 CIRCE_chat = 2
 CIRCE_ver = 7
 CIRCE_rev = 20000426
 /
!>>>>>>>>>>>>>>>>>>>>>>>>>>>>>
 &beam_input
 particle_name = "e+"
 vector_polarization = T
 polarization = 0 -0.6 0
 ISR_on = T
 ISR_alpha = 0.0072993
 ISR_m_in = 0.000511
 CIRCE_on = T
 CIRCE_acc = 2
 CIRCE_chat = 2
 CIRCE_ver =7
 CIRCE_rev = 20000426
 /
```

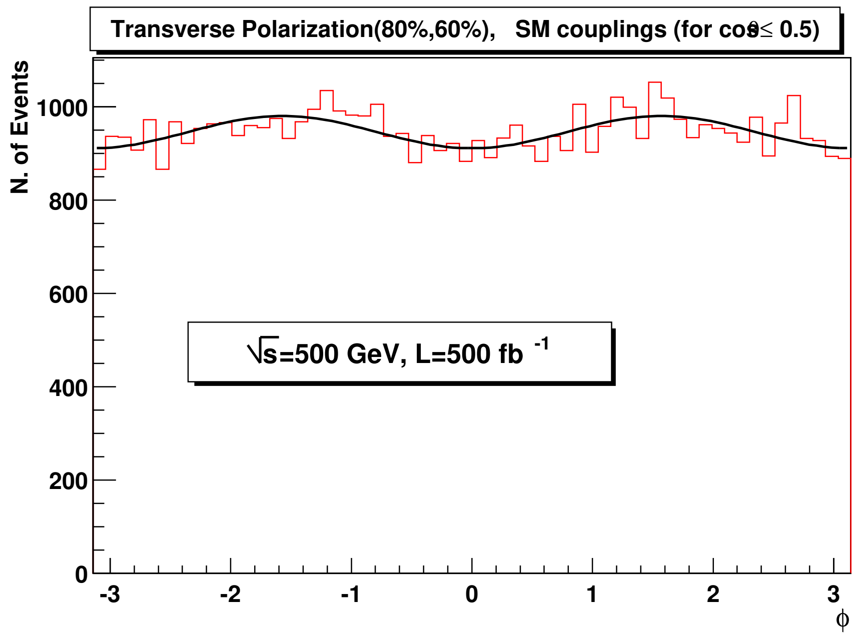

a) SM couplings

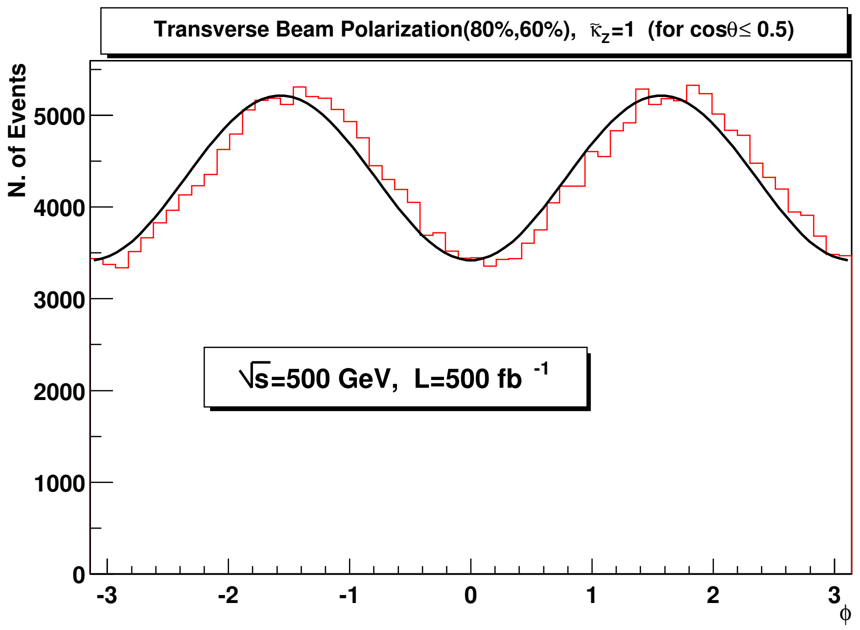

b) $\tilde{k}_Z = 1$

Figure 3: ϕ-distributions for W^- showing the dependence on the ϕ angle. Fig. 3 a) shows the SM distribution. In Fig. 3 b) the distribution corresponding to $\tilde{k}_Z = 1$ is shown. A fitted function shows the phase shift resulting from anomalous CP violating couplings (the phase shift of the fitted function is fixed to the SM phase).

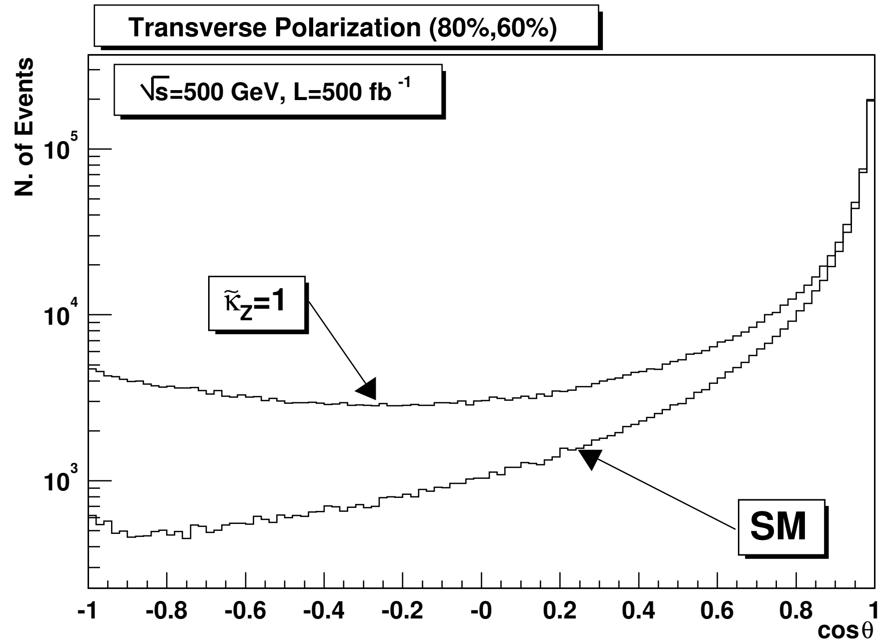

a) Transverse beam polarization.

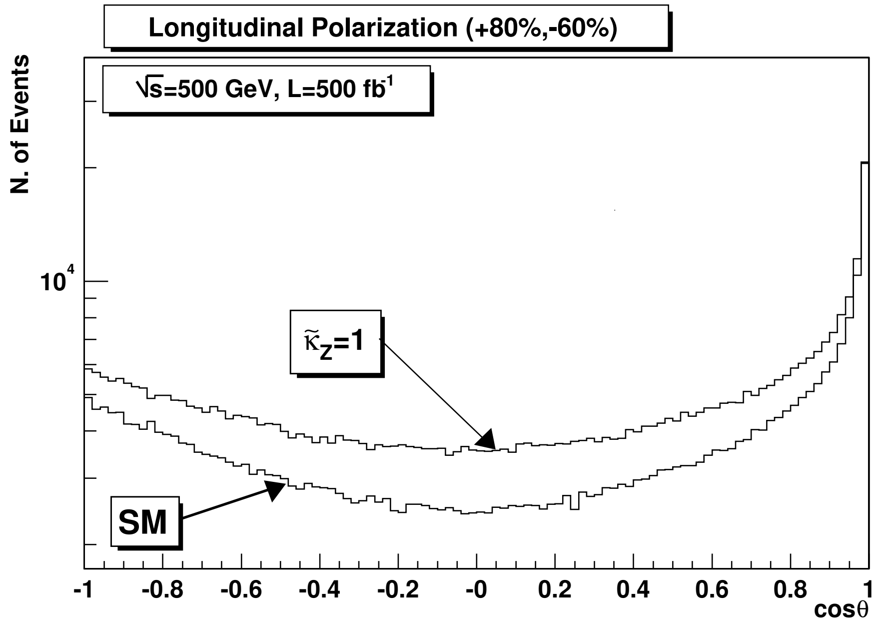

b) Longitudinal beam polarization.

Figure 4: $\cos\theta$-distributions for W^- for transverse and longitudinal beam polarization (comparison between SM couplings and $\tilde{k}_Z = 1$). Here one can observe the change of the cross section for anomalous TGCs.

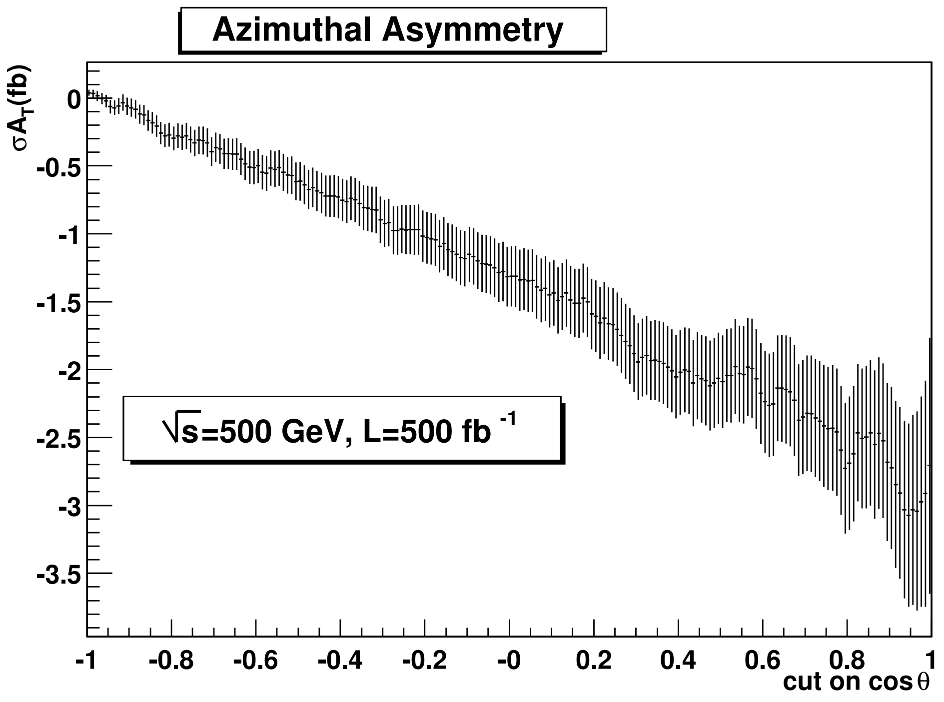

Figure 5: Azimuthal asymmetry σA_T of the ϕ-distribution of the W^- bosons as a function of the cut in $\cos\theta$ (Eq. 4).

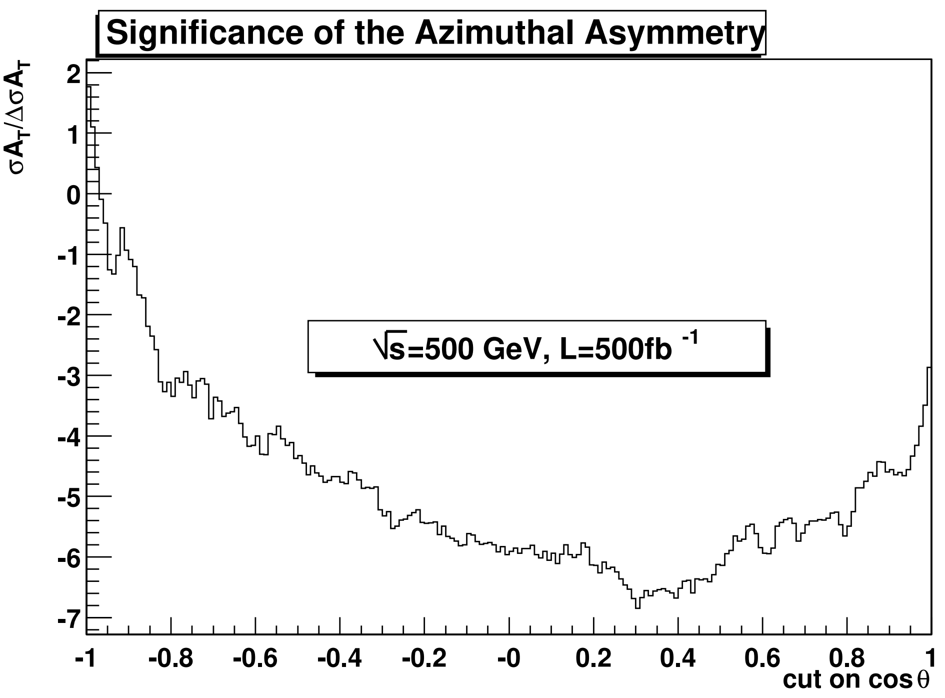

Figure 6: Significance of the azimuthal asymmetry σA_T as a function of the cut in $\cos\theta$ (Eq. 4).

	g_1^γ	g_1^Z	κ_γ	κ_Z	λ_γ	λ_Z	g_4^γ	g_4^Z
1σ-bound from $\cos\theta$ distribution	4.2	6.8	1.0	1.6	3.7	2.4	34.5	29.5
1σ-bound from ϕ distribution	10.7	18.2	25.8	4.4	12.4	4.0	50.2	43.2
1σ-bound from 2D $\cos\theta - \phi$ distribution	4.2	6.9	1.0	1.6	4.1	2.5	35.3	30.1

	g_5^γ	g_5^Z	$\tilde{\kappa}_\gamma$	$\tilde{\kappa}_Z$	$\tilde{\lambda}_\gamma$	$\tilde{\lambda}_Z$
1σ-bound from $\cos\theta$ distribution	32.2	27.4	39.0	33.0	4.9	3.5
1σ-bound from ϕ distribution	46.3	40.3	39.0	34.9	7.1	5.2
1σ-bound from 2D $\cos\theta - \phi$ distribution	34.1	27.7	39.0	33.0	4.6	3.3

Table 1: Expected 1σ-bound $(\times 10^{-3})$ for the case of transverse polarization(80%,60%) with the conditions $\sqrt{s} = 500$ GeV and a luminosity of 500 fb^{-1} . This numbers correspond to the semileptonic decay channel $e^+e^- \longrightarrow W^+W^- \longrightarrow \mu\nu_\mu q_1\bar{q}_2$.

	g_1^γ	g_1^Z	κ_γ	κ_Z	λ_γ	λ_Z	g_4^γ	g_4^Z
1σ-bound from Long.pol.(80%,-60%)	1.9	2.2	0.4	0.5	1.9	1.9	20.3	19.1
1σ-bound from Transv.pol.(80%,60%)	4.2	6.8	1.0	1.6	3.7	2.4	34.5	29.5
1σ-bound from (σA_T) Transv.pol.(80%,60%)	193.0	109.0	4.5	40.0	15.3	10.6	93.0	79.0

	g_5^γ	g_5^Z	$\tilde{\kappa}_\gamma$	$\tilde{\kappa}_Z$	$\tilde{\lambda}_\gamma$	$\tilde{\lambda}_Z$
1σ-bound from Long.pol.(80%,-60%)	18.0	17.4	21.0	20.3	2.2	2.1
1σ-bound from Transv.pol.(80%,60%)	32.2	27.4	39.0	33.0	4.9	3.5
1σ-bound from (σA_T) Transv.pol.(80%,60%)	91.0	82.3	108.0	94.0	11.0	6.5

Table 2: Expected 1σ-bound $(\times 10^{-3})$ for $\sqrt{s} = 500$ GeV and a luminosity of 500 fb^{-1} for the semileptonic decay channel $e^+e^- \longrightarrow W^+W^- \longrightarrow \mu\nu_\mu q_1\bar{q}_2$. This values, except the σA_T numbers, were obtained from the $\cos\theta$ distribution.